Nonlinear Finite Element Analysis of RPC Beams Failing in Shear

Dr.Kaiss F. Sarsam*, Dr. Ihsan A.S. Al-Shaarbaf**
& Maha M. S. Ridha*

Received on: 23/6/2010
Accepted on: 7/4/2011

Abstract

Reactive powder concrete (RPC) is a new type of ultra-high strength and high ductility concrete first developed in the 1990's in France. It is recognized as a revolutionary material that provides a combination of ductility, durability, and high strength. In this research work the nonlinear finite element investigation on the behavior of RPC beams is presented. This investigation is carried out in order to get a better understanding of their behavior throughout the entire loading history. Also, a numerical parametric study was carried out on the RPC beams to investigate the influence of fibrous concrete compressive strength (f'_{cf}), tensile reinforcement ratio (ρ_w), fiber content (V_f) and shear span to effective depth ratio (a/d) on the shear behavior and ultimate load capacity of these beams.

The three- dimensional 20-node brick elements are used to model the concrete, while the reinforcing bars are modeled as axial members embedded within the concrete brick elements. The compressive behavior of concrete is simulated by an elastic-plastic work-hardening model followed by a perfectly plastic response, which terminated at the onset of crushing. In tension, a fixed smeared crack model has been used.

Keywords: Beams, Finite Element, Nonlinear, Reactive Powder Concrete, Shear.

التحليل غير الخطي بطريقة العناصر المحددة لعتبات خرسانة المساحيق الفعالة الفاشلة بالقص

الخلاصة

خرسانة المساحيق الفعالة هي نوع جديد من الخرسانة ذات المقاومة والمطيلية العالية التي تم انتاجها عام 1990 في فرنسا.وقد تم تمييزها كمادة جديدة توفر الترابط بين المطيلية والديمومة والمقاومة العالية. في هذا البحث تم اختبار سلوك عتبات خرسانة المساحيق الفعالة والمعرضة لاحمال القص باستخدام، انموذج التحليل غير الخطي بطريقة العناصر المحددة. هذا الانموذج استخدم للحصول على تفهم افضل لتصرف هذه الاعضاء من خلال تاريخ التحميل الكامل. . كذلك تم إجراء دراسة تحليلية على عتبات خرسانة المساحيق الفعالة, في هذه الدراسة التحليلية درس تأثير محتوى الالياف ، مقاومة الانضغاط للخرسانة ، نسبة حديد التسليح الطولي ، نسبة فضاء القص الى العمق الفعال على سلوك وخواص سعة التحمل القصوى لهذه العتبات . تم استخدام العنصر الطابوقي ذو العشرين عقدة لتمثيل الخرسانة ، اما قضبان التسليح فقد مثلت كعناصر احادية البعد مطمورة في العنصر الخرساني ثلاثي الابعاد ،تم تمثيل تصرف الخرسانة تحت تاثير اجهادات الضغط بالانموذج المرن-اللدن ذو التقوية الانفعالية حيث يتضمن هذا الانموذج افتراض سلوكاً مرناً للخرسانة في مستهل التحميل يعقبه سلوك مرن – لدن عند حدوث التشقق في الخرسانة ،ويستمر تحمل الاجهادات بمعدل انفعال متزايد لحين وصول مرحلة اللدونة التامة، وتنتهي هذه المرحلة بحدوث تهشم في الخرسانة .اما سلوك الخرسانة تحت تاثير اجهادات الشد فقد تم تبني انموذج التشقق المنتشر لتمثيله.

*** Building and Construction Engineering Department, University of Technology/ Baghdad**
**** College Engineering, University of Al-Nahreen / Baghdad**

https://doi.org/10.30684/etj.29.11.7
2412-0758/University of Technology-Iraq, Baghdad, Iraq

Introduction

Reactive powder concrete (RPC) is known as a kind of novel cement-based composite material with ultra-high strength and outstanding performance. Embedding a certain amount of short steel fibers in the matrix can improve the RPC's toughness and overcome the disadvantage of high brittleness. It was originally initiated by a French company BOUYGUES in 1990.Since then, for improved physical and mechanical behaviors, RPC has been rapidly boosted in many application fields ,e.g. civil engineering, hydraulic engineering, mining engineering, bridge construction and military work[(1)].

A number of measures have been adopted, such as eliminating coarse aggregates, reducing water-cement ratio, pressing to shape and heating during curing, to improve interfacial property of cement granules and activate chemical reaction, which turned out ultra-high strength, good toughness and low permeability of RPC. This technique meets the requirement of materials forbuilding large span structures, sky-scrapers, heavily loaded architectures and structures subject to rigorous environments[(2)].

Compressive strength up to 800 MP [(3)]a has been achieved with RPC, Young's modulus of 50 to 60 GPa is common in RPC, as compared with values of 14 to 42 GPa in normal strength concrete. Additionally, the RPC material has a tensile strength ranging between 6 and 13 MPa that is maintained after first cracking for reaching 50 MPa , whereas traditional concrete has tensile strength on the order of 2 to 4 MPa that is lost when cracking occurs[(3)].

The nonlinear finite element analysis of reinforced concrete members is a powerful technique and can supply the researchers with valuable information.

Finite Element Model

In the present research work, a full three-dimensional finite element idealization has been used. This idealization gives accurate simulation for geometry, type of failure and location of reinforcing bars. The 20-node quadratic brick element shown in Fig. (1) is adopted to represent concrete in the present study.

The reinforcement representation that is used in this study is the embedded representation, Fig. (1). The reinforcing bar is considered to be an axial member built into the concrete element. The reinforcing bars were assumed to be capable of transmitting axial force only.

The numerical integration is generally carried out using the 27(3x3x3) point Gaussian type integration rule.

The nonlinear equations of equilibrium have been solved using an incremental-iterative technique operating under load control. The nonlinear solution algorithm that is used in this research work is the modified Newton –Raphson method in which the stiffness matrix is updated at the2nd, 12th, 22nd, ...etc. iterations of each increment of loading .

Material Model Adopted in the Analysis Behavior in Compression:

In compression, the behavior of concrete is simulated by an elastic-plastic work hardening model followed by a perfectly plastic response, which is terminated at the onset of crushing. The growth of subsequent loading surfaces is described by an isotropic hardening rule. A parabolic equivalent uniaxial stress-strain curve has been used to represent the work hardening stage of behavior

and the plastic straining is controlled by an associated flow rule.

The concrete strength under multidimensional state of stress is a function of the state of stress and cannot be predicted by simple tensile, compressive and shearing stress independent of each other. So the the state of stress must be scaled by an appropriate yield criterion to convert it to equivalent stress that could be obtained from simple experimental test. The yield criterion that has been used successfully by many investigators [4],[5] can be expressed as

$$f(\{\sigma\})=(\alpha I_1+3\beta J_2)^{0.5}=\sigma_o \quad \ldots(1)$$

where α and β are material parameters which are dependent on the type of concrete, mainly on the volume fraction of fiber V_f, and their values are shown in Table (1) [6],[7]. I_1 is the first stress invariant and J_2 is the second deviatoric stress invariant. σ_o is an equivalent effective stress at the onset of plastic deformation which can be determined from a uniaxial compression test.

In a reinforced concrete member, a significant degradation in compressive strength can result due to the presence of transverse tensile straining after cracking. In the present study, Vecchio et, al. models are used for HSC [8] members, which illustrates the use of the reduction factor, λ. The compressive reduction factor, λ, for HSC is given as:

$$\lambda = \frac{1}{1+K_c.K_f} \quad \ldots\ldots(2)$$

where K_c is a factor representing the effect of the transverse cracking and straining and K_f is a factor representing the effect of concrete compressive strength f'_c.

$$K_c=0.35\,(\varepsilon_1/\varepsilon_3-0.28)^{0.8} \quad \ldots(3)$$

and

$$K_f = 0.1825\sqrt{f'_c} \geq 1.0 \quad \ldots(4)$$

where ε_1 is the tensile strain in the direction normal to the crack and ε_3 is the compressive strain in the direction parallel to the crack.

Behavior in Tension

In tension, linear elastic behavior prior to cracking is assumed. Cracking is governed by the attainment of a maximum principal stress criterion. A smeared crack model with fixed orthogonal cracks is assumed to represent the cracked sampling point. The post-cracking tensile stress-strain relations, Fig. (2),[9],[10] and the reduction in shear modulus with increasing tensile strain Fig. (3),[11] have been adopted in the present work. The tensile strain at peak tensile stress (ε_{tf1}) is given by:

$$\varepsilon_{tf1} = \varepsilon_t (1 + 0.35\, N_f .d_f .L_f) \quad \ldots\ldots (5)$$

Where

N_f: is the number of fiber per unit area ; given by :

$$N_f = \eta_0 \left[\frac{4V_f}{\pi d_f}\right] \quad \ldots\ldots (6)$$

Behavior of Steel Fiber Reinforced Concrete

In his study, an empirical equations to express the modulus of

$$E_c = 3840\sqrt{f'_{cf}}$$

$$for\ f'_{cf} \geq 25\ MPa \quad \ldots..(7)$$

elasticity E_c For ultra high performance fiber reinforced concrete which suggested by, Graybeal [12] is adopted and is given by: In compression, An empirical equations for peak strain value in uniaxial compression of high strength fiber reinforced concrete (ε_{pf}):

suggested by AL- AZZAWI [13] is adopted in the present study as:

$$\varepsilon_{pf} = 0.00212 + 0.001\, V_f * L_f / d_f \quad ..(8)$$

In his study, an empirical equations to express the uniaxial compressive strength (f'_{cf}) and peak tensile stress (f'_{spf}) for RPC suggested by Ridha [14] is adopted and is given by :

$$f'_{cf} = 3.35\, f'^{0.8}_{c}\, F^{0.05} \quad ....(9)$$

$$f_{spf} = 0.37\, f'^{0.8}_{cf}\, F^{0.2} \quad ....(10)$$

Numerical Example

Description of Test Specimens

A total of 15 RPC beams were tested by Ridha[14] under monotonic loading up to failure. In order to check the validity of the present material model, five of these RPC beams were chosen for this research work to carry out the finite element analysis. These beams were B1,B2, B3,B4 and B5.All tested RPC beams had a longitudinal steel ratio of 3.4% and shear – span/depth (a/d) ratio of 3.5. All RPC beams failed in shear mode. Fig.(4) shows the loading arrangement and reinforcement details. The same type of fibers was used throughout the test program. The fibers were straight, 13mm in length and 0.2mm in diameter making an aspect ratio (L_f/d_f) of 65. The steel fibers had an ultimate tensile strength of 2600 MPa.

Finite Element Idealization and Material Properties:

By making use of the symmetry of loading, geometry and reinforcement distribution of the tested RPC beams, only one half of the length will be considered in the numerical analyses. In the present study, the chosen segments were modeled using 4 brick elements. The finite element mesh, boundary conditions, and loading arrangement are shown in Fig.(5).The dimensions, material properties and the additional material and numerical parameters are listed in Table (2).

The longitudinal bars were simulated as embedded elements into the brick elements. The external loads were applied in equal increments of 5 % of the expected failure load . These increments were reduced at stages close to the ultimate loads. The numerical analyses have been generally carried out using the 27-point integration rule and a convergence tolerance of 2 %.

Results of Analysis

The experimental and numerical load –deflection curves for RPC beams B1 to B5 are shown in Fig.(6). These figures show good agreement for the finite element solution compared with the experimental results throughout the entire range of behavior .They reveal that both the initial and post-cracking stiffnesses are reasonably predicted. The computed failure loads for all RPC beams are close to the corresponding experimental failure load as listed in Table (3).

Parametric Studies

To investigate the effects of some of the material and solution parameters on the nonlinear finite element analysis of RPC beams, beam B5 have been chosen to carry out a parametric study. This study helps to clarify the effect of various parameters that have been considered on the behavior and ultimate load capacity of the analyzed RPC beams.

Influence of Fiber Content

The presence of fibers enhances the ductility and energy absorption capacity of reinforced concrete members and act as crack arresters. Therefore, the addition of a small amount of fibers can increase the flexural, shear and torsional capacity of the members. To study the effect of using different amounts of fibers, four tests have been carried out with

volume fraction of fiber ranging from 2.0% to 3.5%. Fig. (7) shows that the post cracking stiffness and the predicted cracking and ultimate load are considerably increased as the fiber content is increased. The finite element results revealed that an increase up to 13% in ultimate load capacity can be achieved by by increasing (V_f) from 2% to 3.5% as shown in Table (4). Fig. (8) shows the addition of fibers decreases the tensile steel stress in longitudinal bars relative to a 2% fiber content by about 6.7%, 16.5%, and 25.2% for fiber content of 2.5%, 3% and 3.5% respectively.

Effect of Grade of Concrete

In the present research work, a study was made to investigate the use of concrete of higher compressive strength. This was achieved by numerically testing an assumed RPC beams with a wide range of concrete compressive strength. This RPC beam is similar in dimensions, arrangement of reinforcement and other details to B5. The tension stiffening parameters α_1 and α_2 were set equal to 110 and 0.95 respectively. While the shear retention parameters γ_1, $\gamma_2$and γ_3 were set equal to 90,0.9 and 0.1 respectively.

The results of this investigation are shown in Fig. (9). Six grades of concrete were considered in this study. These are125,140,155,170,185 and 200 MPa. The analysis revealed that the failure was due to concrete crushing for all grades of concrete. Therefore the cracking load and post-cracking stiffness are increased by increasing concrete compressive strength. The finite element results revealed that an increase up to 33.9% in ultimate load capacity can be achieved by using compressive strength equal to 200 MPa, compared to a compressive strength of 125 MPa as shown in Table (5). Fig.(10) shows the distribution of longitudinal extreme fiber concrete compressive stresses at P=165 kN along the beam for different values of compressive strength. Stresses obtained from this case study were observed to decrease as the compressive strength is increased. The ratio of decrease in extreme fiber concrete compressive strength was 11.4%, 15.4%, 18.4%, 19% and 20% for 140, 155, 170, 185 and 200 MPa concrete compressive strength relative to $\left(f'_{cf}\right)$ equals to 125 MPa . The figure also reveals that the longitudinal extreme fiber concrete stresses are increased toward the center line of the beam for all values of $\left(f'_{cf}\right)$.

Fig.(11) shows the variation of tensile steel stresses along the span length of beam B5 for different values of the concrete compressive strength $\left(f'_{cf}\right)$ at applied load of 165 kN. It is obvious that as the compressive strength increases the tensile steel stresses slightly decrease.

Influence of Longitudinal Reinforcement

The influence of using different longitudinal reinforcement ratios on the load-deflection curve is investigated. An assumed beam reinforced with various longitudinal reinforcement ratios was numerically tested. The results are shown in Fig. (12). The longitudinal reinforcement ratio varied form 1.4 to 6.7%. The concrete compressive strength and reinforcement yield stress were 110 and 520 MPa respectively. By studying the predicted response of the RPC beam, it can be seen that the increase in the longitudinal reinforcement ratio leads to a stiffer post-cracking response and significant increase in the ultimate load capacity of the RPC beam. The finite element results revealed that an increase up to 122.7% in ultimate load capacity can be

achieved by using longitudinal reinforcement ratio equal to 6.7%, compared to a ratio of 1.4% as shown in Table (6). Fig.(13) shows the distribution of longitudinal extreme fiber concrete compressive stresses along the beam for different ratios of tension reinforcement recorded at applied load = 90 kN. It is obviously shown that the longitudinal extreme fiber concrete stresses decrease with the increase of the steel ratio (ρ_w). The increase in the ratio of tension reinforcement will lead to shift in the neutral axis position downward. This will lead to modified the distribution of extreme fiber concrete compressive stresses in the beam in order to satisfy moment equilibrium, hence a decrease in the extreme fiber concrete stresses occurs. From Fig.(13), it is seen that the longitudinal extreme fiber concrete compressive stresses decrease by a ratio of 13.3%, 23.3%, 25.4%, 27.6% and 31% for 2.4%, 3.4%, 4.4%, 5.4% and 6.4% tensile steel ratio relative to (ρ_w) equal to1.4% for RPC beams.

Fig.(14) shows the variation of tensile steel stresses along the span length of beam B5 for different longitudinal reinforcement ratio (ρ_w). It is clear from this figure that the increase in the longitudinal steel ratio (ρ_w) results in decrease in the tensile steel stresses. The decrease ratio was 26.6%, 48%, 55.9%, 62.2% and 67.2% for 2.4%, 3.4%, 4.4%, 5.4% and 6.4% tensile steel ratio relative to (ρ_w) equal to 1.4%.

Influence of shear span-depth ratio a/d

In order to investigate the influence of using different shear span-depth (a/d) ratio on the behavior of load-deflection curve of the RPC beams, an assumed beam reinforced with various shear span-depth (a/d) ratios were numerically tested. The results are shown in Fig. (15). The shear span-depth (a/d) ratio varied form 1.5 to 5.

By studying the predicted response of the beam, it can be seen that the increase in the shear span-depth (a/d) ratio leads to a decrease in the post-cracking stiffness response and significant decrease in the cracking load and ultimate load capacity of the beam. The finite element results revealed that an decrease up to 70.4% in ultimate load capacity can be achieved by increasing (a/d) ratio from 1.5 to 5 as shown in Table (7). Fig.(16) shows the distribution of longitudinal extreme fiber concrete compressive stresses along the beam for different ratio of shear span to effective depth (a/d) at applied load = 110 kN. It is obviously shown that the longitudinal stresses increase with the increase of the shear span to effective depth ratio (a/d) the increase in the ratio of shear span to effective depth (a/d) will lead to increase in the moment for a given loading level. Hence an increase in compressive stresses occurs. From Fig.(16) , it is seen that the longitudinal extreme fiber concrete compressive stresses increase by a ratio of 50%, 104%, 146%, 195%, 257.7%, 313.5% and 412.4% for 2, 2.5, 3, 3.5, 4, 4.5 and 5 shear span to effective depth ratio (a/d) relative to a/d = 1.5 for RPC beam B5 .

Fig. (17) shows the variation of tensile steel stresses along the span length for different shear span to effective depth ratio (a/d) for RPC beams. It is clear from this figure that the increase in the shear span to effective depth ratio (a/d) results in an increase in the tensile steel stresses. The increase ratio was 104.7%, 234.9%, 451.3%, 524.2%, 688.1%, 781.4% and 783.3% respectively, for 2, 2.5, 3, 3.5, 4, 4.5 and 5 shear span

to effective depth ratio relative to a/d = 1.5.

Conclusions

1.The three-dimensional finite element model adopted in the present work, is suitable to predict the behavior of RPC beams failing in shear. The numerical results were in good agreement with the experimental load-deflection curves of the tested RPC beams throughout the entire range of behavior. The mean value (μ) of ($P_{u,Num.}$ / $P_{u,Exp.}$) is 0.974 with standard deviation (SD) of 0.0676 and coefficient of variation (COV) of 6.93%.

2. The cracking load and post-cracking stiffness of the load- deflection curve increased by increasing the concrete compressive strength$\left(f'_{cf}\right)$. When $\left(f'_{cf}\right)$ increases from 125 MPa to 200 MPa, the ultimate load capacity increases by 26.7% and the longitudinal compressive stresses decreases by 20%.

3. The effect of increasing the amount of tension steel bars (ρ_w) on the load-deflection behavior of RPC beams has been studied numerically. The increase of the amount of ρ_w causes an increase in the post-cracking stiffness of the load- deflection curve and leads to a higher ultimate load. When ρ_w increases from 1.4% to 6.4% the ultimate load capacity increases by 113.3%, while the longitudinal extreme fiber concrete compressive stress decreases by 31% and the tensile steel stress decreases by 68%.

4. The increase in the amount of fibers V_f causes an increase in the post-cracking stiffness of the load-deflection curve. The finite element solutions show that when V_f increases from 2% to 3.5% the ultimate load capacity increases by 13%, the longitudinal extreme fiber concrete compressive stress decreases by 25.2% and the tensile steel stress decreases by 17%.

5. The effect of increasing the shear span to effective depth ratio (a/d) on the load-deflection behavior of RPC beams has been studied numerically. It is obvious that the increase in (a/d) results in a decrease in the post-cracking load-deflection response and the predicted ultimate load. When a/d ratio increases from 1.5 to 5, the ultimate load capacity decreases by 70.4% and the longitudinal extreme fiber concrete compressive stress increases by 412.4%.

References

[1] Yao, Z. X., Zhou, J., "Study on Fracture Energy of Reactive Powder Concrete Reinforced by Steel-Polypropylene Hybrid Fiber",Journal Built Mater (in Chinese),Vol.8, No.4, 2005, PP.356-360.

[2] Yang, J. U., YuDan, J. I. A., HongBin, L. I. U. and Jian, C. H. E. N., "Mesomechanism of Steel Fiber Reinforcement and Toughening of Reactive Powder Concrete", Science China Series E-Technological Science, Vol.50,No.62007,PP.815-832.

[3]Collepardi,S., Coppola, L., Troli, R. and Collepardi,M.,"Mechanical Properties of Modified Reactive Powder Concrete", In: V-M. Malhotra Ed. Proceedings Fifth CANMET/ACIInternational Conference on Superplasticizers and the Chemical Admixtures in Concrete, Rome, Italy, and Farmington Hills, MI: ACI Publication SP-173, 1997, pp.1-21.

[4]Thannon, A. Y., "Ultimate Load Analysis of Reinforced Concrete Stiffened Shells and Folded Slabs Used in Architectural Structures", Ph.D. Thesis, University of Wales, Swansea, 1988.

[5]Hinton, E. and Owen, D.R.J., "Finite Element Software for Plates and Shells" Pineridge Press, Swansea, 1984.

[6] Allose, L. E., "Three Dimensional Nonlinear Finite Element Analysis of Steel Fiber Reinforced Concrete Beams in Torsion", M.Sc. Thesis, University of Technology, 1996.

[7]Abdul-Wahab H.M.S., "Strength of reinforced concrete corbels with fibers ", ACI Structure J.,Vol.86,No.1, Jan.-Feb. 1989,pp.60-66.

[8]Vecchio T, Collins F. J., and Aspioties M. P., "High Strength Concrete Elements Subjected to Shear", ACI Structural Journal, July-Aug. 1994, pp. 423-433.

[9]Al-Shaarbaf, I. A.S., "Three Dimensional Nonlinear Finite Element Analysis of Reinforced Concrete Beams in Torsion", Ph.D. Thesis, University of Bradford, 1990.

[10]Al-Moussely, B. S., "Three Dimensional Nonlinear Finite Element Analysis for Steel Fiber Reinforced Concrete Beams Subjected to Combined Bending and Torsion", M.Sc. Thesis, University of Technology, 1998.

[11]Naji, J. H., and I.May, "The Effect of Some Numerical and Material Parameters on the Nonlinear Finite Element Analysis of Reinforced Concrete Beams", Proceedings of the Third Arab Engineering Conference, Vol. 1, March 1998, No. 5 , pp. 10-17.

[12] Graybeal, B., and Davis, M., "Cylinder or Cube: Strength Testing of 80 to 200 MPa (11.6 to 29 ksi) Ultra-High-Performance Fiber –Reinforced Concrete", ACI Materials Journal, V.105, No.6, Nov-Dec, 2008, pp. 603-609.

[13] Al-Azzawi , Z. M. K. , "Capacity of High Strength Fiber Reinforced Beam Column Joints ", M. Sc. Thesis , University of Technology , 1997 .

[14] Ridha , M. M. S. , " Shear Behavior of Reactive Powder Concrete Beams" , PhD Thesis , University of Technology , Baghdad , 2010 , PP 204.

Nomenclature

f'_c	uniaxial compressive strength of nonfibrous RPC.
f'_{cf}	uniaxial compressive strength of fibrous RPC.
f_{spf}	uniaxial splitting tensile strength of fibrous RPC.
, α_2	tension-stiffening parameters
β	material constant
	shear retention factor
$_1$, γ_2 , γ_3	shear retention parameters
λ	compressive strength reduction factor of concrete
σ_n	stress normal to cracked plane.
ε_n	strain normal to cracked plane
ε_{cr}	cracking strain
σ_{cr}	cracking stress.

Table (1): Material Parameters.

V_f	α	β
0.0	0.3546798 σ_o	1.3546798
0.5	1. 0993042 σ_o	2.0993042
1.0	1. 4960526 σ_o	2.4900526
1.5	1 .7960526 σ_o	2.7960526
2.0	2.0960526 σ_o	3.0960526

Table (2): Dimensions, material properties and the additional material and numerical paraeters us* Assumed values

Beam Designation	B1	B2	B3	B4	B5
Fiber Content (%)	0.0	0.5	1.0	1.5	2.0
Shear Span a (mm)	392	392	392	392	392
Width b (mm)	100	100	100	100	100
Effective Depth d (mm)	112	112	112	112	112
Concrete					
Young's Modulus, E_c (GPa)	39.10	42.25	44.20	46.80	48.80
Compressive Strength , f'_{cf} (MPa)	78	94	98	103	110
Tensile Strength, f_{spf} (MPa)	5.5	9.2	11	14.5	15.4
Poisson's Ratio , ν *	0.15	0.15	0.15	0.15	0.15
Steel					
Young's Modulus, E_S (MPa)	200000	200000	200000	200000	200000
Longitudinal Bars					
Steel Ratio ρ_w (%)	3.14	3.14	3.14	3.14	3.14
Yield Stress f_y (MPa)	520	520	520	520	520
Tension-Stiffening Parameter					
α_1	10	80	90	100	110
α_2	0.4	0.7	0.8	0.9	0.95
Shear Retention Parameters					
γ_1	20	60	70	80	90
γ_2	0.4	0.6	0.7	0.8	0.9
γ_3	0.1	0.1	0.1	0.1	0.1

- **f'_{cf}, f_{spf}, and E_c = Experimental value d for Ridha's RPC beams.**

Table (3): Comparison between experimental and predicted failure loads.

Beams	Experimental Failure Load $P_{u,Exp}$ [14] (kN)	Numerical Failure Load (kN)	
		$P_{u,Num}$	$\frac{P_{u,Num.}}{P_{u,Exp.}}$
B1	71	74	1.042
B2	133	127	0.955
B3	140	137	0.979
B4	155	153	0.987
B5	165	162	0.982

Table (4): Numerical Ultimate Load Capacity of Beam B5 for Different Volume Fractions of Steel Fibers (V_f)

Fiber Content V_f (%)	2	2.5	3.0	3.5
Ultimate Load (kN)	162	170	176	183
Percentage of Increasing in Ultimate Load (%)	0	4.9	8.6	13

Table (5) Numerical Ultimate Load Capacity of beam B5 for Different Value of Concrete Compressive Strength (V_f = 2.0%)

Compressive Strength (MPa)	125	140	155	170	185	200
Ultimate Load (kN)	177	187	199	217	226	237
Percentage of Increase in Ultimate Load (%)	0	5.6	12.4	22.6	27.7	33.9

Table (6): Numerical Ultimate Load Capacity of Beam B5 for Different Longitudinal Steel Ratio(ρ_w)%, (V_f = 2.0%).

Longitudinal Steel Ratio ρ_w (%)	1.4	2.4	3.4	4.4	5.4	6.4
Ultimate Load (kN)	97	137	162	192	205	216
Percentage of Increasing in Ultimate Load(%)	0	41.2	67	97.9	111.3	122.7

Table (7): Numerical Ultimate Load Capacity of Beam B5 for Different Shear Span to Effective Depth Ratio (V_f = 2.0%).

Shear Span to Effective Depth Ratio (a/d)	1.5	2.0	2.5	3.0	3.5	4.0	4.5	5.0
Ultimate Load (kN)	378	281	227	187	162	142	125	112
Percentage of Decreasing in Ultimate Load(%)	0	25.7	39.9	50.5	57.1	62.4	66.9	70.4

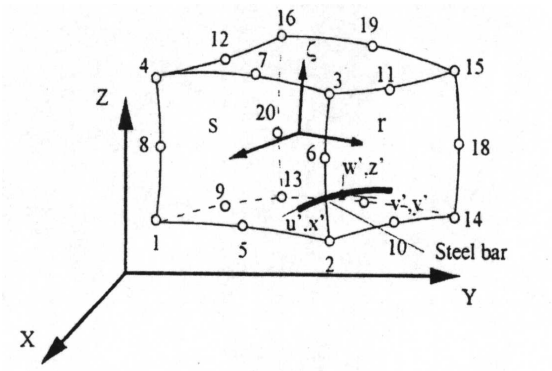

Figure (1) The twenty-node brick element.

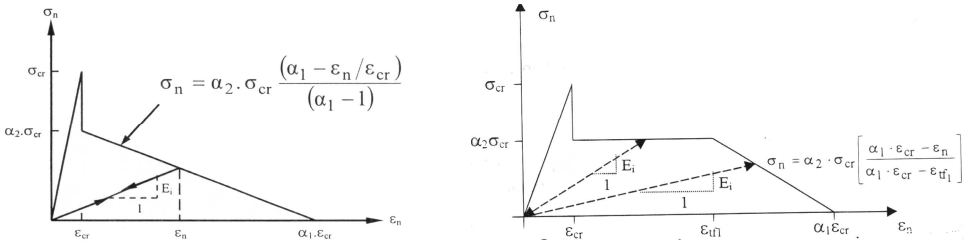

a) Plain concrete b) Fiber reinforced concrete[10].

Figure (2) Post-cracking models for cracked concrete[10].

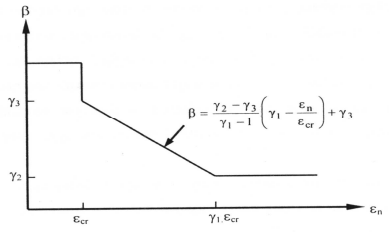

Figure (3) Shear retention model for cracked concrete. [9]

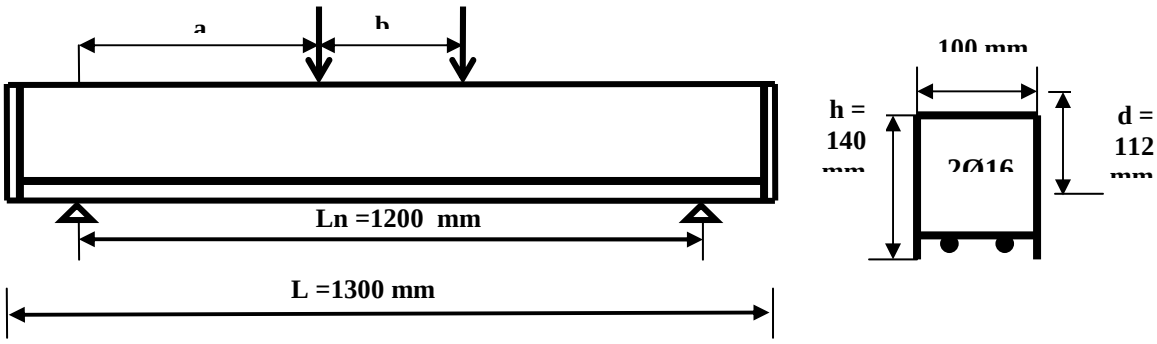

Figure (4).Dimensions and reinforcement details of Ridha's RPC beams [14] {All dimensions in (mm)}

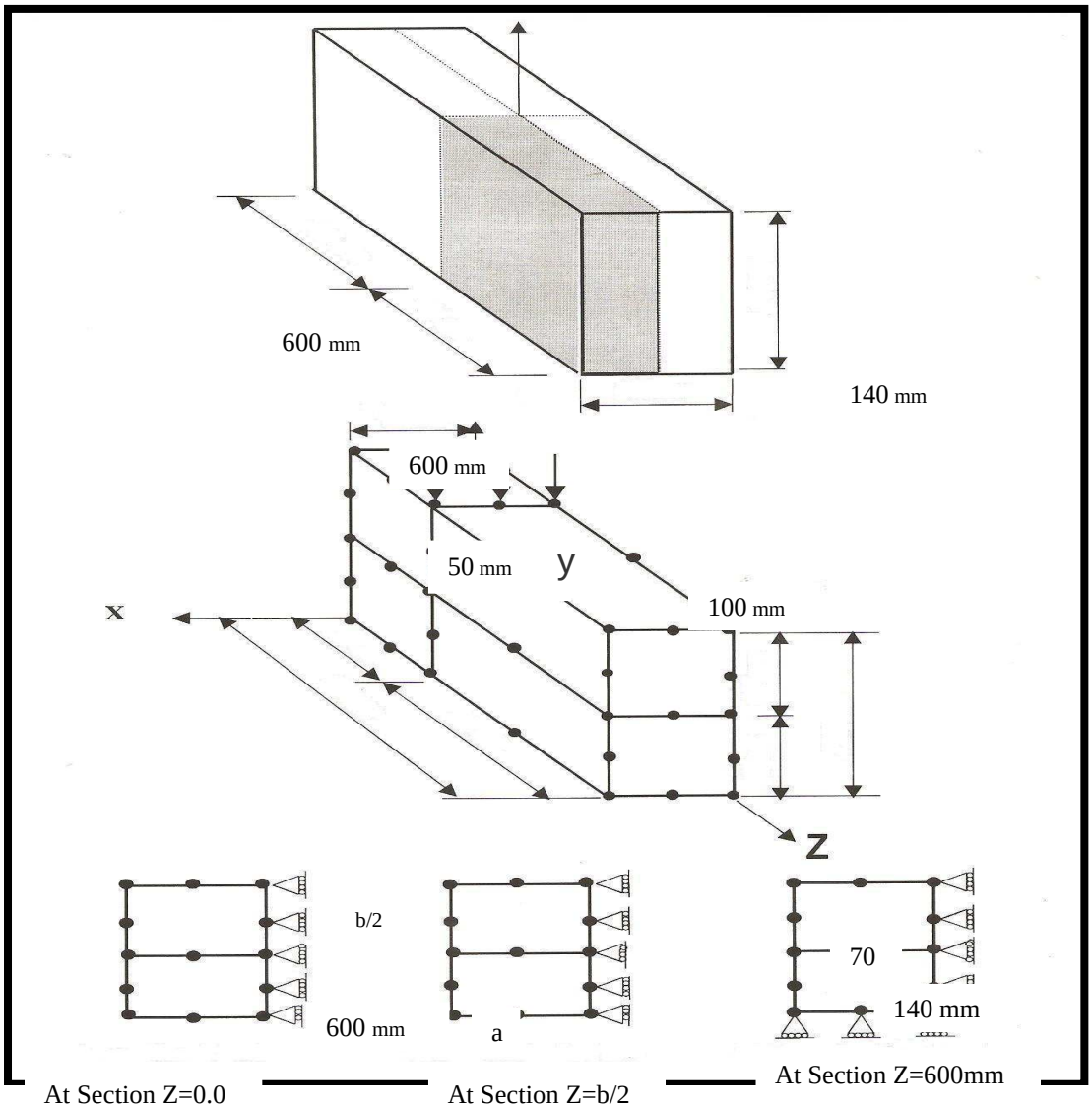

Figure (5). Finite element mesh and conditions for Ridha's RPC beams. {All dimensions in (mm)}

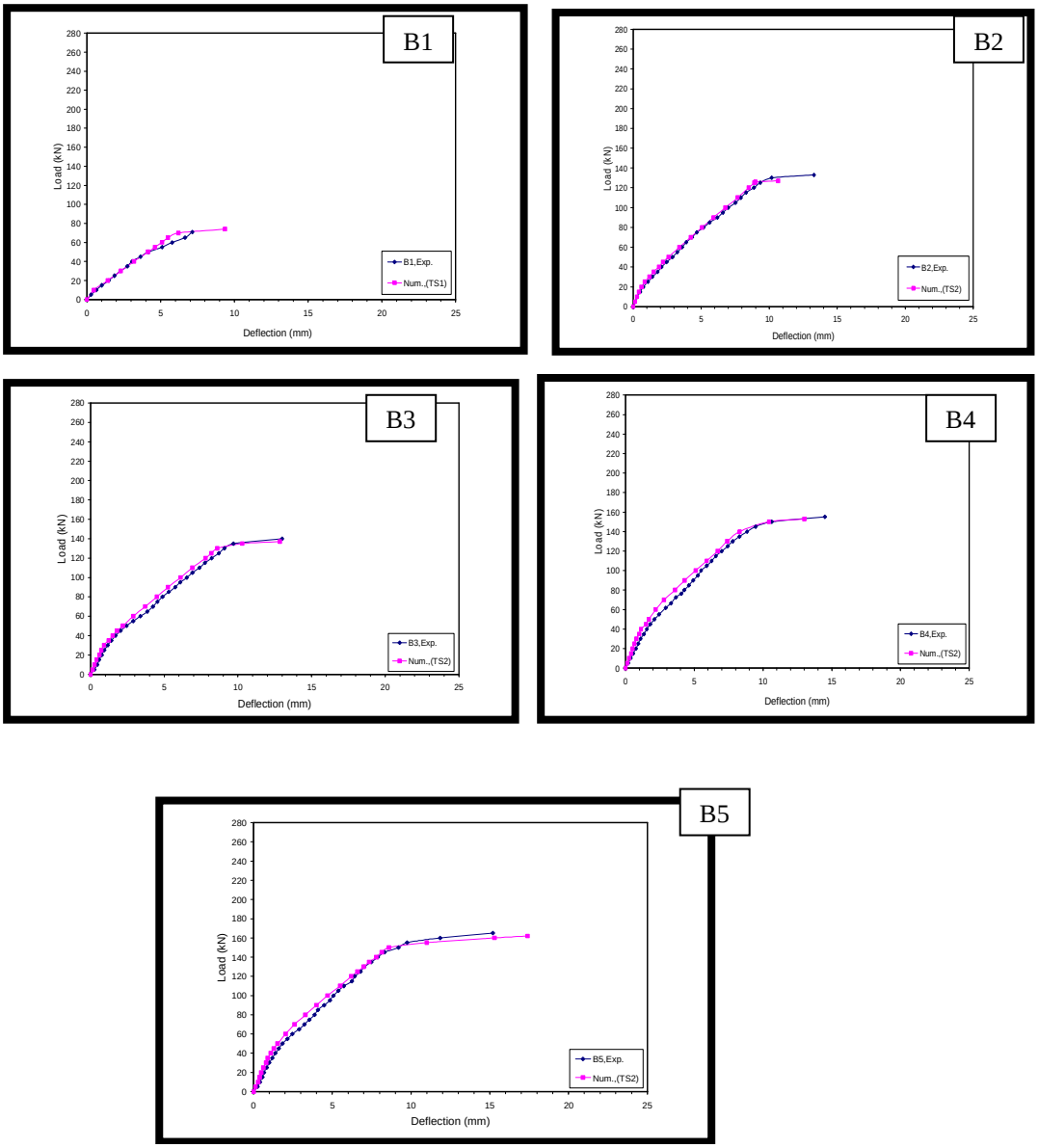

Figure (6): Beams B1,B2,B3,B4 and B5, Experimental and Numerical Load- Midspan Deflection Curves.

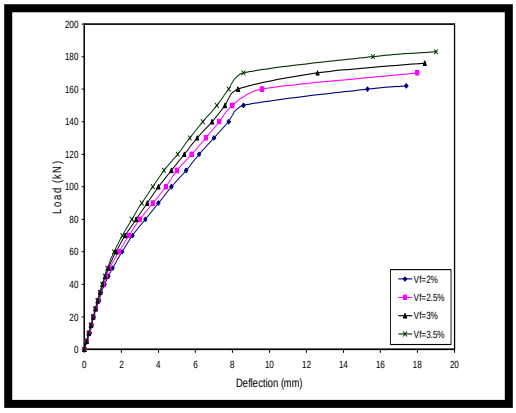

Figure (7): Effect of (V_f) on Numerical Load-Midspan Deflection Curves of RPC Beams.

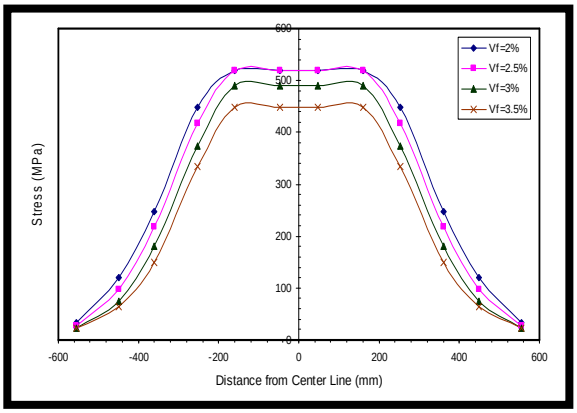

Figure(8): Effect of Fiber Content (V_f) on the Numerical Tensile Steel Stresses ofBeam B5, at Applied Load=160 kN.

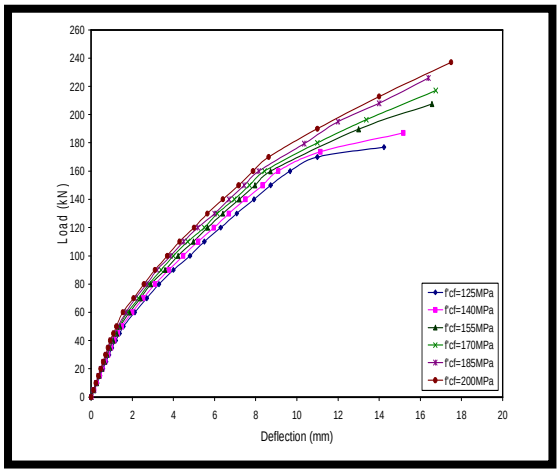

Figure(9): Effect of (f'_{cf})on the Numerical Load- MidspanDeflection Curves of RPC Beam B5.

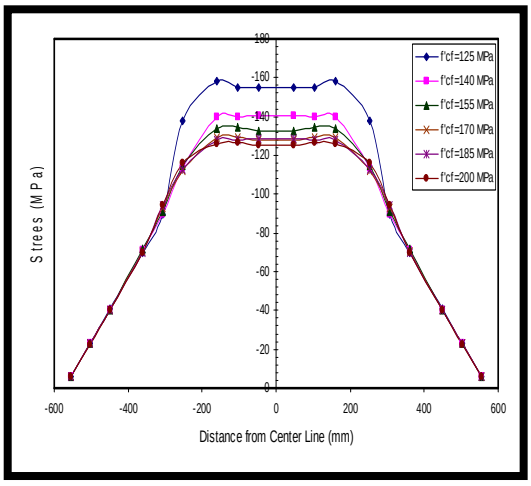

Figure(10): Distribution of the Longitudinal Extreme Fiber Concrete Compressive Stresses Along Beam B5 at Applied Load=165 kN